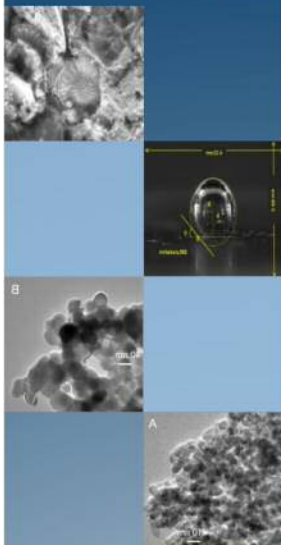


2012



RECENT DEVELOPMENTS IN METALLURGY, MATERIALS AND ENVIRONMENT

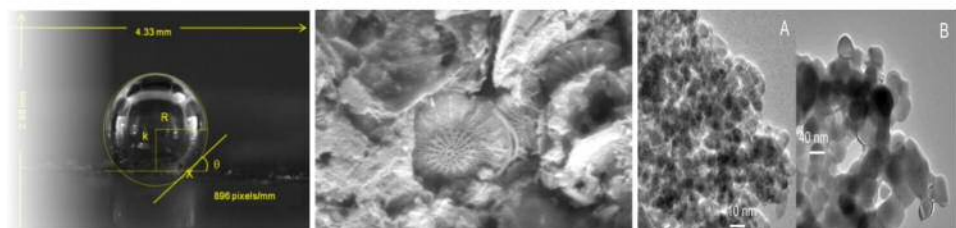
CHAPTER 14

Purification of Kaolin Clays by Means of Electrochemical Techniques

Flores Segura J. C., Reyes Cruz V. E., Legorreta García F., Hernández Cruz L.E. and Veloz Rodríguez M. A.

ÁREA ACADÉMICA DE CIENCIAS DE LA TIERRA Y MATERIALES, INSTITUTO DE CIENCIAS BÁSICAS E INGENIERÍA DE LA UNIVERSIDAD AUTÓNOMA DEL ESTADO DE HIDALGO

ISBN 978-607-9023-18-8



Materials

CHAPTER 14

Purification of Kaolin Clays by Means of Electrochemical Techniques

Flores Segura J. C., Reyes Cruz V. E., Legorreta García F., Hernández Cruz L.E.,
and Veloz Rodríguez M. A.

Área Académica de Ciencias de la Tierra y Materiales, Instituto de Ciencias Básicas e Ingeniería de la Universidad Autónoma del Estado de Hidalgo, Ciudad Universitaria, Carretera Pachuca-Tulancingo Km. 4.5, Mineral de la Reforma Hidalgo; C.P. 42184, México.

Abstract

In the present work a kaolin clay sample was studied and its treatment was carried out with the purpose of separating iron oxides contained in it. This kaolin clay comes from Agua Blanca de Iturbide in Hidalgo State (Mexico). The clay was classified and treated to obtain micrometrical particles. This material in solution was studied by voltammetry, this solution showed a cathodic process attributed to reduction of iron in kaolin. Likewise, a subsequent process of macroelectrolysis at a controlled cell potential, showed that, when process is finished, iron is solved; helping to increase the purity of kaolin. The mineral original was characterized by X-ray diffraction (XRD), particle size analysis (PSA), scanning electron microscopy (SEM) and chemical analysis by high dispersion spectroscopy of inductively coupled plasma (ICP). The obtained product after treatment was characterized by ICP.

Keywords: Clays; Kaolin; Purification; Electrochemistry

1. Introduction

The kaolin is a clay product from decomposition of feldspar rocks, it is a silicate of hydrate of aluminum whose main component is the kaolinite, its formula is $2\text{H}_2\text{O}\bullet\text{Al}_2\text{O}_3\bullet 2\text{SiO}_2$, it has a wide application in several industries; its consumption at world level was estimated for 2013 by Freedonia

Group on 24.8 million metric tons. Big locations exist in countries such as: United States, England, Brazil, Indonesia, China, etc., where kaolin is extracted and treated to purify it, and then to take maximum advantage of its properties [1].

In Mexico there are also important mineral veins, mainly in states of Veracruz, Guanajuato, and Hidalgo [2]. In Hidalgo there is a vein in the municipality of Agua Blanca de Iturbide [3], where kaolin presents an important quantity of impurity, which degrades its value and its properties (mainly its whiteness due to iron oxides) [4].

Wet purification process, done in most of plants where kaolin clays are treated around the world, includes mechanical methods as extraction, degritting, mixed, classified, decanted and dried [1], some or the combination of the following ones: high intensity magnetic separation, flotation, lixiviation and flocculation [4-9].

Within the purification processes those that have acquired greater importance are: lixiviation process which consists on treating kaolin with acids in order to reduce iron oxides content and this way to whiten the polluted clays [7, 9], and that of flotation which consists on adding a hydrophobic surfactant to kaolin solution and to make pass air bubbles that catch the impurities [6, 8]. The application of several purification techniques causes the increase of the costs for its treatment [2].

Claudio Camesselle and collaborators in 2007 [10] found that application of electric potential in combination with use of oxalic acid in an electroremediation cell, helps to whiten kaolin increasing its whiteness to 80%, besides minimizing the quantity of reagents used in common treatment of purification for kaolin clays. The electroremediation process consists on placing a moistened soil between two holes with an electrolyte, so the transport mechanisms caused by application of an electric field concentrate pollutants on some of electrodes, these mechanisms are: electroosmosis, electromigration, electrophoresis, and diffusion.

The results obtained by Camesselle reveal that the electrochemical processes can be an alternative to confront the problem of purification of polluted kaolin. However, these studies also indicate that high energy consumption is required in the process when creating fronts with low pH.

For this reason, in the present investigation the problem is approached carrying out characterization and electrochemical studies of a solution of kaolin clay coming from the municipality of Agua Blanca, Hidalgo. It is necessary to mention that the application of these techniques in an electrolytic cell represents a decrease in the quantity of used energy, in comparison with the electroremediation treatment.

The kaolin clay was first mechanically processed until obtaining micrometrical particles. These particles were carried into solution. The corresponding voltammetric study was performed and also a chronopotentiometric study with the solution of kaolin clay in an electrolytic cell, with the purpose of knowing energy conditions on which iron oxides decrease. With the information obtained from these studies, it was carried out a macroelectrolysis study with the kaolin clays solution in order to carry out the removal of iron oxides.

2. Experimental procedure

Mechanical preparation consisted on wet sieve of the kaolin clay (from Agua Blanca, Hidalgo and marketed by the company “Molinos y Moliendas de Pachuca”) with sieve -400 mesh to obtain particles with a smaller size of 37 μm . X-Ray diffraction was carried out with Inel X-ray diffractometer, model Equinox 2000, with radiation source Cu-K α . Sample was dried at 120 °C. It was pulverized in an agate mortar and prepared in the equipment sampler. Clay morphology was observed by means of a scanning electron microscope, brand Jeol, model JSM 6300. The sample dried off at 120 °C was previously covered with gold. For the analysis of particle size, a small quantity of sample was placed in deionised water and it was exposed to ultrasonic bath during 3 min, then it was processed by means of analyzer of particle size by laser ray diffraction brand Beckman Coulter, model LS13320.

For chemical analysis, samples were digested with HF and H₃BO₃. Then, they were analyzed with an inductively coupled plasma spectrometer, brand Perkin Elmer, model Optima 3000XL.

For electrochemical study the techniques of cyclic voltammetry and chronopotentiometry were used and were done in an electrochemical cell of 3 electrodes. The electrodes used are: as working electrode a silver badge, as counterelectrode a DSA and as reference electrode SCE. The solution used for the voltammetric study was kaolin clays at 25% of solids in quantities of 300 mL. In the performing of electrochemical studies a potentiostat-galvanostat PAR263A was used. The techniques were applied through equipment software.

For macroelectrolysis study a power source brand GW Instek and 2 electrodes were used with a cell potential obtained from chronopotentiometric study.

3. Results and discussions

3.1 Characterization of the kaolin clay

Diffractogram of analyzed kaolin clay is described in Figure 1. The sample presents a high kaolynite content (JCPDS 01-078-1996) and, quartz (JCPDS 03-065-0466) in its main phases.

On the other hand, it is corroborated that this clay possesses an important quantity of impurities among those highlight the maghemite and iron or titanium oxides, being iron oxides those that contribute to the beige-reddish coloration to clays, when they are in significant quantities.

In Figure 2 the results obtained from analysis of particle size by laser ray diffraction are shown.

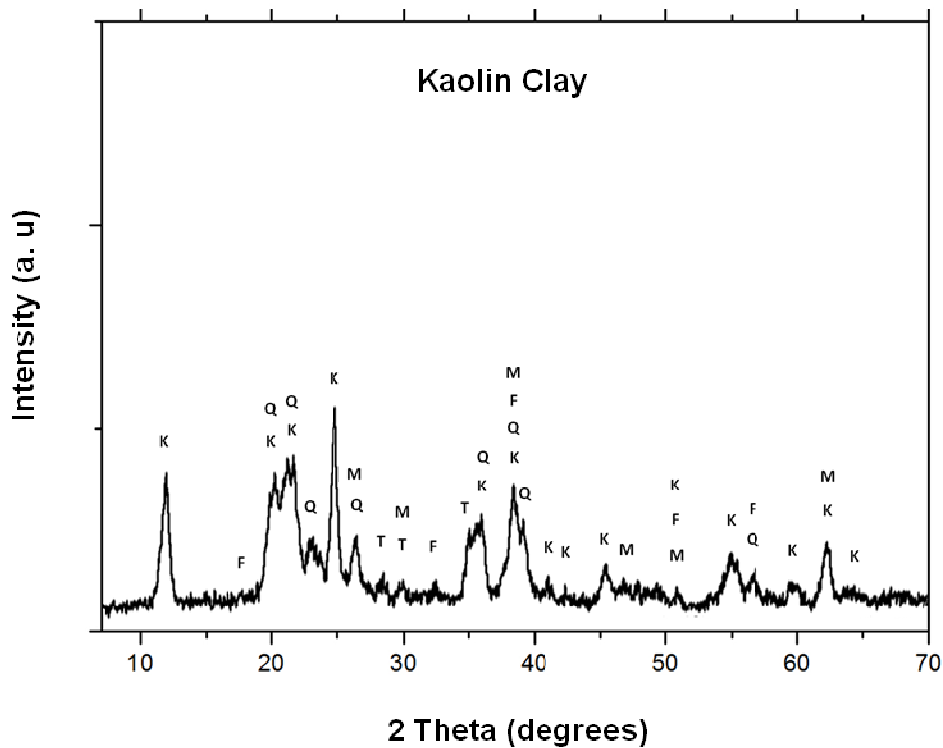


Figure 1. Diffractogram of X-ray for kaolin clay from the municipality of Agua Blanca, Hidalgo. (K=kaolynite; Q=quarz; M=Maghemite; T=titanium oxides; and F= iron oxides).

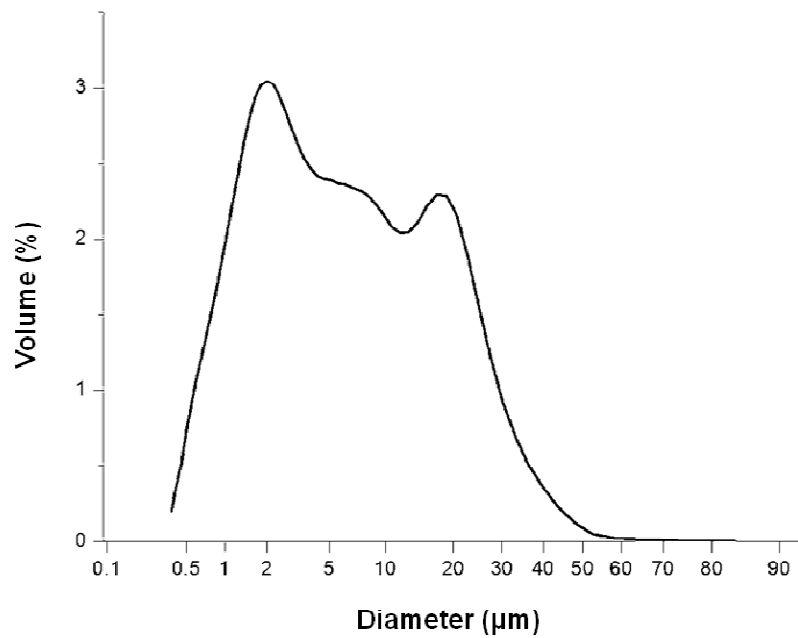


Figure 2. Distribution of particle size for the kaolin clay.

In Figure 2 two populations of main particles are observed, one with size of approximately $2\mu\text{m}$ that occupies the biggest percentage in the volume of the sample. The second majority population corresponds to particles with size of approximately $20\mu\text{m}$, although the presence of particles can also be appreciated with sizes up to $60\mu\text{m}$ and more. These sizes can be presented due to the loads of the fine particles causing interactions between them and forming accumulations of major size. This corresponds with that observed in the microscopy images obtained by scanning electron microscopy (SEM).

In Figure 3 microscopy of kaolin sample is presented. It was obtained with the SEM looking for accumulations of kaolin of major sizes, between 30 and $60\mu\text{m}$.

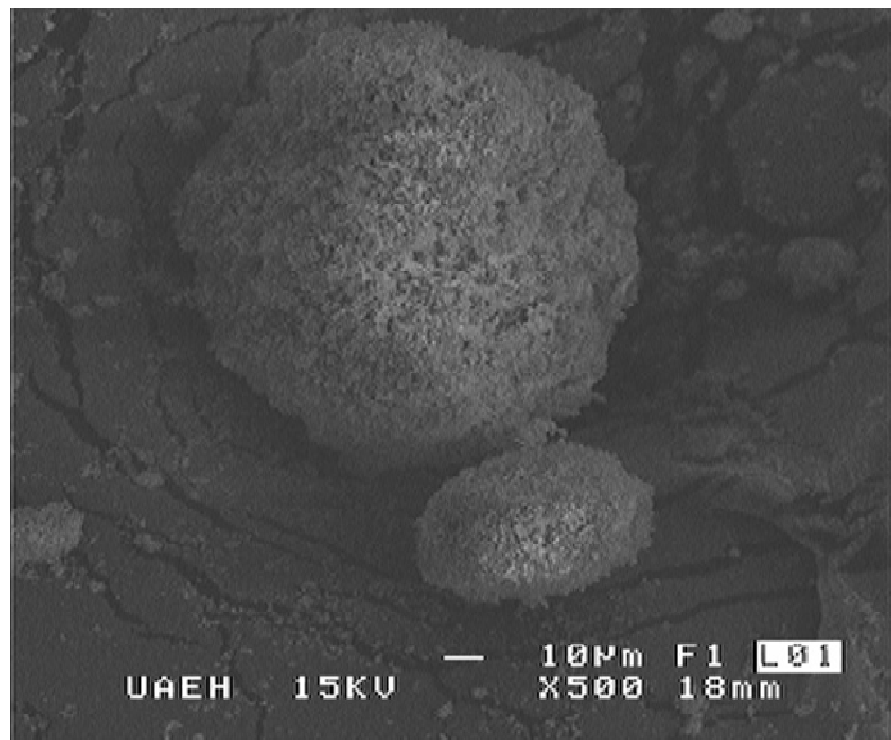


Figure 3. Microscopy of kaolin clay obtained with SEM.

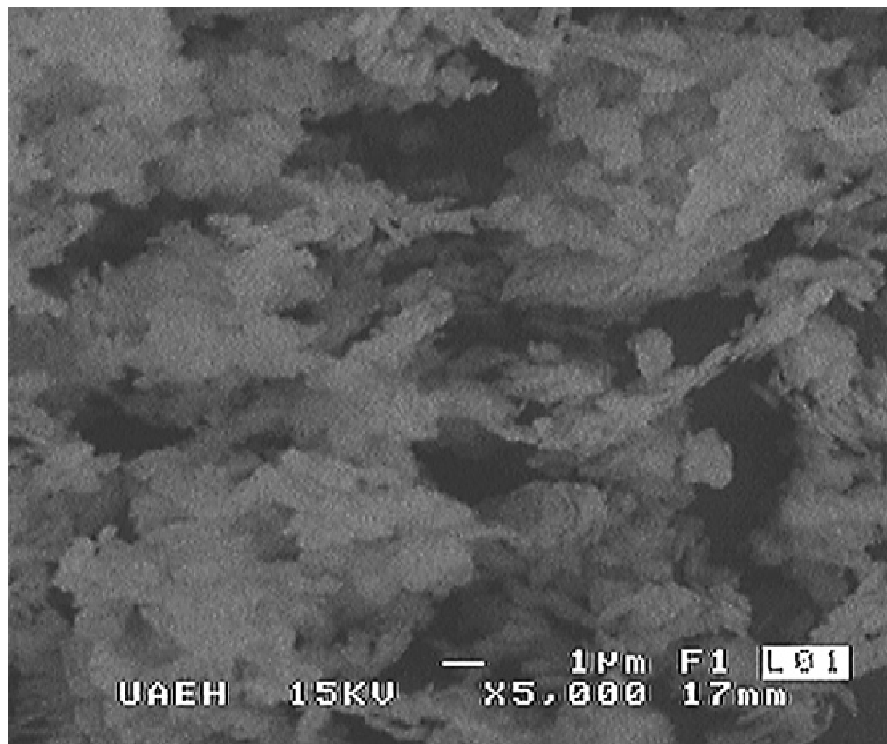


Figure 4. Microscopy of the kaolin clay obtained with the (SEM) at 5000 increases.

In Figure 4, the same sample of that in Figure 3 is observed, with more magnification although in low resolution. In the figure it is possible to observe stacking of plates which is characteristic of kaolinite.

The obtained results of chemical analysis, Table 1, show high contents of iron and titanium. Also, the proportion in weight observed between alumina (Al_2O_3) and silica (SiO_2) does not correspond with the formula of kaolinite, which is 1:2, this is due to the quartz presence in excess. It is assumed that all alumina present is forming part of the kaolinite.

% Wt			
Fe_2O_3	TiO_2	Al_2O_3	SiO_2
0.6834	0.6934	23.3334	18.8347

Table 1. Chemical composition of the sample of kaolin clay from Agua Blanca de Iturbide, Hidalgo, Mexico, obtained after acid digestion.

3.2 Electrochemical studies

In Figure 5 voltammetric response of kaolin solution is shown. It was performed at a scanning speed of 20 mV s^{-1} when the scanning begins in cathodic direction.

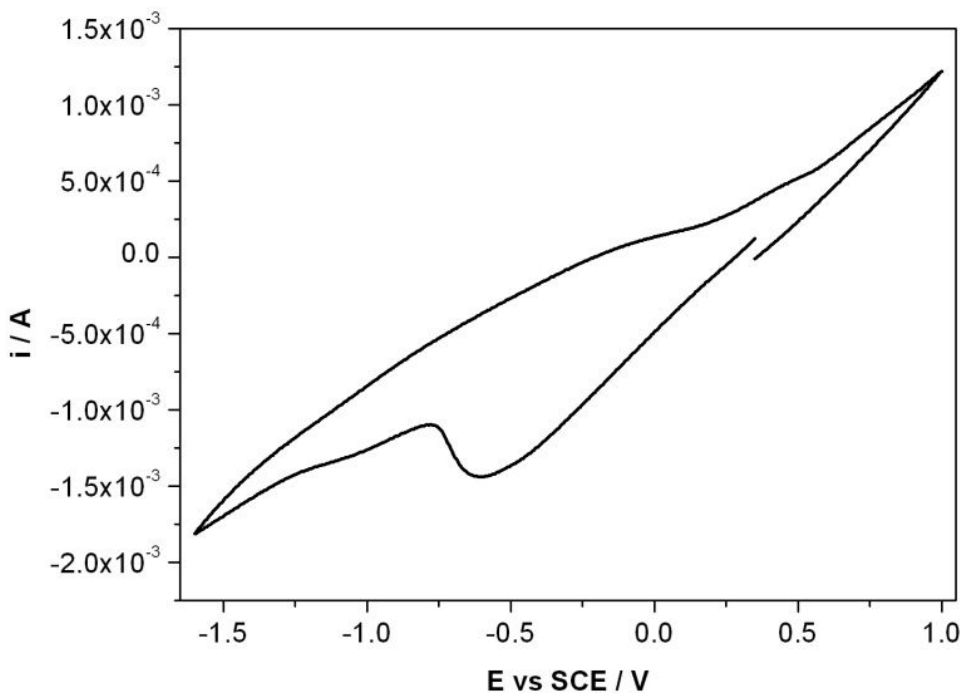


Figure 5. Voltammogram obtained on a surface of Ag in a kaolin (from Agua Blanca) solution to a scanning speed of 20 mVs^{-1} .

In Figure 5 two reduction processes are observed, one in the potential range of 0.280 to -0.780 V vs SCE and the other in the range of -0.780 to -1.6 V vs SCE. The first process is attributed to the reduction of iron species present in kaolin and the second to reduction of the medium. When the potential scanning is inverted, an oxidation process is observed, which begins at -0.167 V. This is attributed to the oxidation of the reduced products of the kaolin in the direct scanning.

These results indicate that reduction of iron present in kaolin could be carried out in the potential range between 0.28 and -0.780 V and at a current range from 0 to $-1.46 \times 10^{-3} \text{ A}$.

In order to knowing the cell potential that should be used in an electrochemical arrangement of two electrodes, a chronopotentiometric study was carried out. The figure 6 shows the chronopotentiometric transient of kaolin reduction when a current of $-1.46 \times 10^{-3} \text{ A}$ is imposed to the Ag electrode.

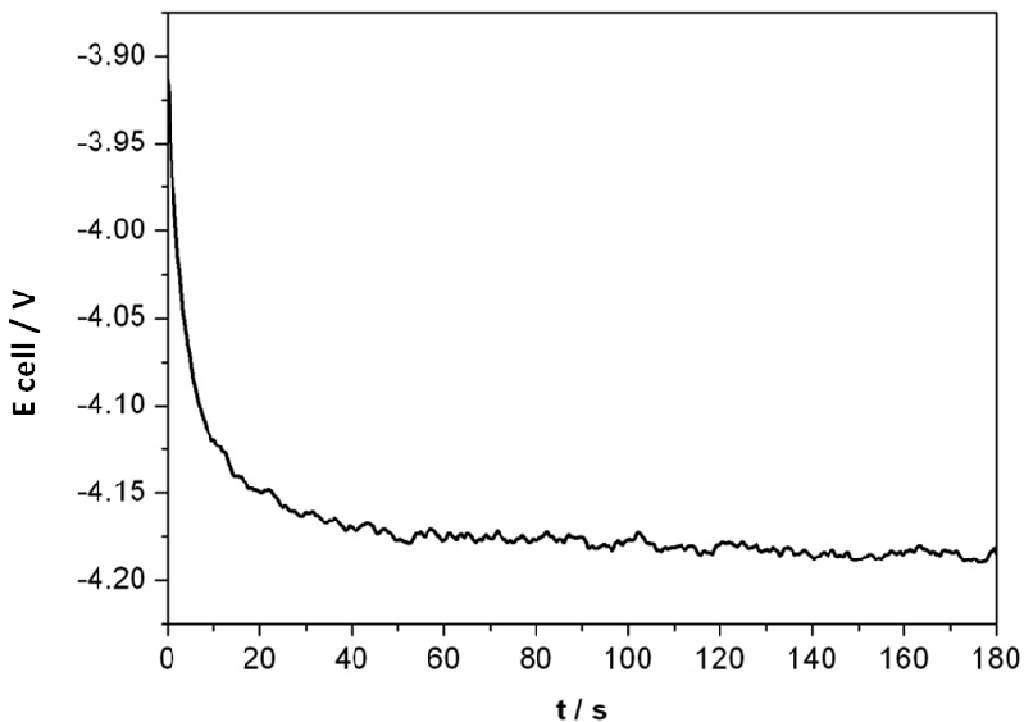


Figure 6. Chronopotentiometric transient obtained on a Ag surface in a kaolin (from Agua Blanca) solution when a current of $-1.46 \times 10^{-3} \text{ A}$ was imposed.

In the figure 6, a considerable decrease of the cell potential is observed up to -4.16 V vs SCE in the interval of time from 0 to 30 s. At times greater than 30 s a constant potential is presented for the rest the electrolysis time. This behaviour indicates that only one species is being reduced and that it is not being finished in the solution; in this case the species is attributed to the iron oxide.

With the information of these results the process of macroelectrolysis of kaolin was carried out to obtain a higher transformation of iron reduced species present in the mineral.

In Table 2 are shown the results from chemical analysis with inductively coupled plasma (ICP) carried out to kaolin samples subjected to macroelectrolysis when a cell potential is imposed in the interval from 3.5 to 4.3 V.

APPLIED POTENTIAL	IRON OXIDE CONTENT ANALYZED	PERCENTAGE OF IRON OXIDE REMOVED
0V	0.6834	0
3.5V	0.6156	9.91850
3.7V	0.5859	14.2717
3.9V	0.5760	15.7075
4.1V	0.5656	17.2363
4.3V	0.5797	15.1689

Table 2. Results of the analyses carried out to kaolin samples subjected to macroelectrolysis when a cell potential is imposed in the interval from 3.5 to 4.3 V.

In Table 2 it is observed that as the cell potential increases the quantity of iron oxides present in the sample diminishes, until certain point. It is observed clearly that when increasing the cell potential from 3.5 V there is a tendency to decrease of content of iron oxides, until a maximum on 4.1 V. This is the cell potential given in the chronopotentiogram of the solution. This corroborates that iron oxides are the species decreasing in the kaolin. Once this point is overpassed, at 4.3 V, it is assumed that the reduction of the medium is also beginning, causing decrease in the reduction of the iron oxides. It is important because controlling the cell potential the quantity of iron oxides removed could be greater giving place to the obtaining of kaolin with more purity degree.

4. Conclusions

The results obtained by chemical analysis and XRD of kaolin clay indicated that a high kaolynite content is present, besides the quartz and impurities, these mainly from iron and titanium oxides. The microscopies obtained by SEM revealed the presence of particles with sizes bigger than 30 μ m, even though in their majority they correspond to fine particles, this was corroborated with the analysis of particle size that showed great extent of micrometrical particles with size of 2 μ m approximately.

The electrochemical studies (voltammetry and chronopotentiometry) showed that solution of micrometrical kaolin particles has a good response to reduction processes of the species present in this mineral. The potential interval where the species of iron in the kaolin decrease was located from 3.5 to 4.3 V.

The chemical analyses with coupled plasma after macroelectrolysis at controlled cell potential indicated that the electrochemical techniques are a viable alternative to purify the kaolin because as the potential increases the quantity of removed iron increased, achieving in this first studies a 17% of iron oxides removing.

Acknowledgements

The authors wish to thank to FOMIX-HIDALGO for the economic support for this research and to the Área Académica de Ciencias de la Tierra y Materiales of the Universidad Autónoma del Estado de Hidalgo for the infrastructure support without which it would not be possible the performing of the studies.

The author Juan Carlos Flores Segura thanks to CONACyT for the scholarship to carry out its doctorate studies.

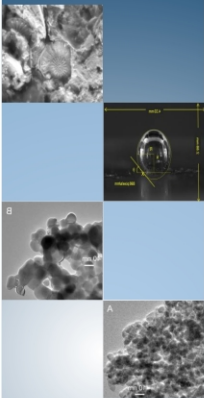
References

1. H. H. Murray. (2006), *Applied clay mineralogy. Ocurrences, processing and application of kaolins, bentonites, palygorskite-sepiolite, and common clays*. Elsevier. Reino Unido.
2. S. E. Coordinación General de Minería.(2010), *Anuario estadístico de la minería mexicana ampliada 2009*. Coordinación General de Minería No. 39, ISBN 970-9897-14-4, México.
3. FIFOMI (2004). *Inventario físico de los recursos minerales del municipio de agua blanca, Hgo*. CRM. México.
4. S. Chandrasekhar y S. Ramaswamy. "Influence of mineral impurities on the properties of kaolin and its thermally treated products", *Applied Clay Science*, No. 21 (2002) pp. 133-142.
5. Dirección General de Promoción Minera (2007). *Perfil de mercado de caolín*. Coordinación General de Minería. México.
6. P. Raghavan et al. "Value addition o paper coating grade kaolins by the removal of ultrafine coloring impurities". *International journal of mineral processing*, No. 50 (1997) pp. 309-316.
7. N. J. Saikia et al. "Characterization, beneficiation and utilization of a kaolinite clay from Assam, India". *Applied clay science*, No. 24 (2003) pp. 93-103.
8. A.B. Luz y A. Middea. "Purification of kaolin by selective flocculation". *43rd Annual conference of metallurgist of CIM*, ISBN-10 1894475496, Hamilton, Ontario, Canada, Agosto 22-25 (2004). pp. 243-253.
9. R. Asmatulu. "Removal of the discoloring contaminants of east georgia Kaolin clay and its dewatering". *Turkish J. Eng. Env. Sci*, No. 26 (2002) pp. 447-453.
10. C. Cameselle et al. "Electrokinetic Bleaching of Kaolin Clay", *6th Symposium on electrokinetic remediation*, Depósito Legal: VG-586-2007, Vigo, España, Junio 12-15. (2007) pp. 133-134.

For further information contact:

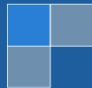
Juan Carlos Flores Segura: carlosflores.segura@gmail.com

2012



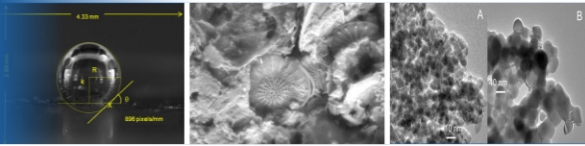
RECENT DEVELOPMENTS IN METALLURGY, MATERIALS AND ENVIRONMENT

*Martin I. Pech-Canul
Ana L. Leal-Cruz
Juan C. Rendón-Angeles
Carlos A. Gutiérrez-Chavarría
Jorge López-Cuevas
José L. Rodríguez-Galicia*
Editors



ISBN: 978-607-9023-18-8

A standard one-dimensional barcode representing the ISBN number.



CONTENIDO

PREFACIO

ii

Capítulo	METALURGIA EXTRACTIVA	Página
1	Oxidación Acuosa de los Productos de la Reducción de Calcopirita <i>O. J. Solis-Marcial, G.T. Lapidus-Lavine</i>	1
2	Lixiviación Reductiva de Lodos de Manganeso <i>M. Gutiérrez-Muñoz, V.H. Brito-Ramos, E. Pérez-Anacleto, I. Pérez-Cruz, G.T. Lapidus-Lavine</i>	12
3	Lixiviación Oxidante de Minerales Tipo Sulfuros Empleando Microondas y Ozono <i>F. R. Carrillo-Pedroza, M. J. Soria-Aguilar, E. T. Pecina-Treviño, P. Aguilar-Morua</i>	23
4	Efecto del MgO y Mg(OH)₂ en la Tostación y Lixiviación de un Mineral Refractario de Oro y Plata <i>J. H. Coronado- López, J. L. Valenzuela-García, A. Valenzuela-Soto, M. A. Encinas-Romero</i>	34
5	Molienda Ultrafina como Pretratamiento antes de Cianurar un Mineral Refractario de Oro <i>J.A. González Anaya, F. Nava-Alonso, E.T. Pecina-Treviño</i>	45
6	Dependencia de la Temperatura y Estudio Termodinámico de Oro Contenido en Soluciones Base Tiosulfato <i>G. Juárez L., I. Rivera L., F. Patiño C., E. Salinas R., J. Hernández A., M. Pérez L., E. Yescas M. y R. Martínez M</i>	56
7	Extracción de Plata de Soluciones Ácidas de Tiourea con el Ácido bis(2-etilhexil) Ditiofosfórico <i>Z. Gamiño-Arroyo, A. Buch, D. Pareau, M. Avila-Rodríguez, L.E. Sánchez-Cadena, A.R. Uribe Ramírez, M. Stambouli</i>	67

8	Separación Selectiva de la Esfalerita, Pirlita y Cuarzo en el Circuito de Flotación de Zinc	78
	<i>Gloria I. Dávila Pulido, Alejandro Uribe Salas, Fabiola C. Nava Alonso</i>	
9	Capacidad de Adsorción y Despojamiento de Zinc Presente en Solución Acuosa, Utilizando la Resina Quelante, Dowex M-4195	89
	<i>Martínez Meza, Ramona Guadalupe, Almazán Holguin, Luis Alonso</i>	
10	Eficiencia Energética del Proceso de Remoción de Zinc a partir de Escorias	100
	<i>G. González Múzquiz, J. Jiménez Ramírez, J. L. Rodríguez Galicia</i>	
11	Eficiencia Energética de Horno de Producción de Zinc a partir de Blenda Tostada	111
	<i>G. González Múzquiz, J. Jiménez Ramírez, J. L. Rodríguez Galicia</i>	

MEDIO AMBIENTE

12	Aislamiento de Microorganismos de Efluentes Mineros	122
	<i>C. E. Jaramillo-Gómez, O. Monge-Amaya, M.T. Certucha-Barragán, E. Acedo-Felix, F. J. Almendariz-Tapia</i>	
13	Activación de Zeolitas en un Horno Solar para su Aplicación en la Remoción de Micotoxinas	133
	<i>G. T. Munive, A. L. Leal-Cruz, J.L. Servín-Rodríguez, J. Varela-Salazar, M. I. Pech-Canul, J. A. Rodríguez-García y E. Rocha-Rangel</i>	
14	Recuperación de Estroncio de Aguas Residuales por el Proceso Electroquímico con Electrodos de Hierro y Análisis Termodinámico	144
	<i>Gregorio González Zamarripa, José R. Parga Torres, Víctor M. Vázquez Vázquez</i>	

15	Efecto de los Parámetros del Proceso de Activación de Chabasita sobre la Remoción de Flúor	155
	<i>J.L. Servín-Rodríguez, A. L. Leal-Cruz, G. C. Tiburcio-Munive, M.I. Pech-Canul, J. A. Rodríguez-García y E. Rocha-Rangel</i>	
16	Cinéticas de Flotación para la Remoción de Cromo por Flotación Iónica	166
	<i>L. Morales Damián, M. Caudillo González, E. Elorza Rodríguez, J. L. Quiroga Velázquez</i>	
17	Aplicación de un Diseño de Experimentos Factorial 2³ para el Estudio de la Cinética de Remoción de Iones Cromo con Wollastonita Natural a Partir de Soluciones Sintéticas de Cromo (VI) en Medio Ácido	177
	<i>M.A. Encinas-Romero, L. A. Núñez-Rodríguez, A. Gómez-Álvarez</i>	
18	Recuperación del Complejo Oro Tiosulfato Utilizando Guanidina en una Resina de Intercambio Aniónico	188
	<i>M. E. Chaparro-Félix, J. L. Valenzuela-García, G. Tiburcio-Munive, J. R. Parga-Torres, S. Aguayo-Salinas</i>	

MATERIALES

19	Recubrimiento Biomimético de Ferritas para el Tratamiento de Cáncer por Hipertermia	199
	<i>E.M. Múzquiz-Ramos, D.A. Cortés-Hernández, J.C. Escobedo-Bocardo, M.A. Aguilar-González, J.G. Osuna-Alarcón</i>	
20	Modelación Matemática de Temperatura para la Deposición de Partículas de Fe-Cr-Mo sobre Acero D2 por HVOF	210
	<i>C. A. Guevara Chávez, J. L. Acevedo Dávila, P. Hernández Gutiérrez, F. Cepeda Rodríguez</i>	

21	Análisis Mediante el Método de Elementos Finitos del Comportamiento Térmico, Mecánico y Microestructural en la Unión de Soldadura Multi-pasos GMAW de Placas de Acero Hardox 400 y ASTM 514	221
	<i>F. Cepeda Rodríguez, J. L. Acevedo Dávila, E. D. Aguilar Cortez, C.A. Guevara Chávez, P. Hernández Gutiérrez</i>	
22	Efecto de los Parámetros de Proceso en la Formación de Al₄C₃ durante la Soldadura Láser de Nd:YAG en Compuestos Avanzados de Aluminio-Grafito	232
	<i>E. D. Aguilar-Cortes, F. J. García-Vázquez, J. L. Acevedo-Dávila, F. Cepeda-Rodríguez, M. I. Pech-Canul</i>	
23	Efecto de la Velocidad de Avance y Mezcla de Gases de Protección en la Penetración y Propiedades Mecánicas Durante la Fabricación de Tubería de Acero Inoxidable 304L por el Proceso GTAW	243
	<i>P. Hernández-Gutiérrez, J. L. Acevedo-Dávila, J.J. Ruiz Mondragón, C.A. Guevara Chavez¹, F. Cepeda-Rodríguez</i>	
24	Determinación de la Estructura Cristalina del Sulfualuminato de Estroncio Sr₄Al₆O₁₂SO₄	254
	<i>J. A. Rodríguez-García, E. Rocha-Rangel, J. M. Almanza Robles, J. Torres Torres, A. L. Leal Cruz, T. Munive G</i>	
25	Preparación y Sinterización de Polvos Finos de SrTiO₃ Mediante la Transformación de Mineral de Celestita Bajo Condiciones Hidrotérmicas	265
	<i>Y. M. Rangel-Hernández, J. C. Rendón-Angeles, Z. Matamoros-Veloza, M. I. Pech-Canul, K. Yanagisawa</i>	
26	Purificación de Arcillas de Caolín Mediante Técnicas Electroquímicas	276
	<i>Flores Segura J. C., Reyes Cruz V. E., Legorreta García F., Hernández Cruz L.E., y Veloz Rodríguez M. A.</i>	

27	Caracterización y Estudio de Separación Gravimétrica de Arenas de Arcillas Caoliníticas Procedentes de Agua Blanca de Iturbide, Hidalgo (México)	287
	<i>Legorreta-García F., Olvera-Venegas P.N., Hernández-Cruz L.E., Bolarín-Miró Ana M. y Sánchez De Jesús F.</i>	
28	Síntesis In-Situ de Materiales Refractarios Base CaAl₂O₄ a Partir de Diferentes Materias Primas	298
	<i>E. Rocha-Rangel, J.A. Rodríguez-García, E. Refugio-García, J.G. Miranda-Hernández, J.M. Almanza-Robles y J. Torres-Torres</i>	
29	Evaluación Microestructural de Materiales de Al₂O₃-ZrO₂-SiO₂	309
	<i>G.I. Vázquez Carbajal, J.L. Rodríguez Galicia, J.C. Rendón Ángeles, J. López Cuevas, C.A. Gutiérrez Chavarría</i>	
30	Cintas Porosas de Circón Obtenidas por el Método de Colado en Cinta	320
	<i>M. León-Carriedo, C. A. Gutiérrez-Chavarría, J. L. Rodríguez-Galicia, J. López-Cuevas</i>	
31	Soldadura Compuesta con Matriz de SnAgCu Reforzada con Partículas de CuAlAg	331
	<i>S.B. Castro Salinas, J. García Rocha</i>	
32	Influencia de la Composición de la Aleación de Aluminio sobre la Variabilidad del Ángulo de Contacto en substratos de SiC	342
	<i>M. Montoya-Davila, R. Escalera-Lozano, M. I. Pech-Canul and M. A. Pech-Canul</i>	
33	Influencia de las Fases de Reforzamiento sobre el Comportamiento de Corrosión de Compósitos Al/SiC en NaCl 0.1M	353
	<i>R. Escalera-Lozano, M. Montoya-Dávila, M.A. Pech-Canul, M.I. Pech-Canul</i>	

34	Comportamiento de la Corrosión de una Aleación Al-17%Si-14% Mg en Disoluciones de Cloruros	364
	<i>M.A. Pech-Canul, M.I. Pech-Canul, J.M. Guevara Vela, V. M. Ugalde Saldívar³, J.C. Aguilar, E.E. Coral-Escobar</i>	
35	Fabricación de Aleaciones Al-Zn-Mg Resistentes a la Corrosión usando Reciclaje de Ánodos de Baterías Alcalinas Descargadas y Latas de Aluminio	375
	<i>R. M. Ochoa Palacios, J. Torres Torres, A. Flores Valdés, J. M. Almanza Robles</i>	
36	Formación de Aluminatos de Estroncio por Reacción en Estado Sólido de Mezclas SrCO₃-Al₂O₃ con Activado Mecánico	386
	<i>J. Torres Torres, R. Saldaña Garcés, A. Flores Valdés</i>	
37	Propiedades Mecánicas de Materiales Compósitos del Sistema Binario Ba_{0.75}Sr_{0.25}AlSi₂O₈-ZrO₂, Sintetizados por Reacción en el estado Sólido a Partir de Materias Primas Activadas Mecánicamente	397
	<i>M.V. Ramos-Ramírez, J. López-Cuevas, J.L. Rodríguez-Galicia</i>	
		408
38	Síntesis por Reacción en el Estado Sólido de Celsiana de Estroncio a Partir de Mezclas de SrCO₃, Al₂O₃ y Ceniza Volante Activadas Mecánicamente	
	<i>C.M. López-Badillo, J. López-Cuevas, S. Díaz de la Torre</i>	
39	Reemplazo Parcial del CaO por BaO en Muestras Vitrocerámicas del Sistema SiO₂-Al₂O₃-CaF₂-RO (R = Ca, Mg, Ba)	419
	<i>M. Garza-García, J. López-Cuevas, C.A. Gutiérrez-Chavarría, N. Piedad-Sánchez, E. Camporredondo-Saucedo</i>	